

**Figure 6.** Plot of magnetic susceptibility vs. temperature for  $\text{Ta}_2\text{NiSe}_7$ : (solid line) raw data; (dashed line) data corrected for paramagnetic impurities.

( $-1.54 \times 10^{-7}$  emu  $\text{g}^{-1}$ ) and are typical of a diamagnetic material (dashed curve in Figure 5). If, however, the data are corrected for ion-core diamagnetism,<sup>23</sup> the resulting susceptibility is small but positive ( $3.3 \times 10^{-5}$  emu  $\text{g}^{-1}$ ).

Four-probe single-crystal conductivity measurements along the needle axis, *b*, show that  $\text{Ta}_2\text{NiSe}_7$  exhibits metallic behavior over the temperature range 100–300 K, with a room-temperature conductivity of  $310 \Omega^{-1} \text{cm}^{-1}$  (Figure 6). In this temperature range the material exhibits no metal-insulator transition as occurs at 140 K in  $\text{FeNb}_3\text{Se}_{10}$ .<sup>24</sup> The electrical conductivity is indicative of a material with a partially filled band at the Fermi level. Since the material is diamagnetic, the paramagnetism that arises from this partially filled band is small when compared with the ion-core diamagnetism. Because of the difficulty in obtaining large single crystals, the conductivity of the Pt compound has not been measured.

While  $\text{Ta}_2\text{NiSe}_7$  has a structure similar to that of  $\text{FeNb}_3\text{Se}_{10}$ , the properties of these two compounds are very different and parallel those of the corresponding trichalcogenides. Thus,  $\text{FeNb}_3\text{Se}_{10}$  is metallic and paramagnetic and displays charge density wave phenomena similar to those of  $\text{NbSe}_3$ ,<sup>25</sup> while

(23) Klem, W. Z. *Anorg. Allg. Chem.* **1941**, *246*, 347–362.

(24) Hillenius, S. J.; Coleman, R. V.; Fleming, R. M.; Cava, R. J. *Phys. Rev. B: Condens. Matter* **1981**, *23*, 1567–1575.

(25) Bullet, D. W. *J. Phys. C* **1982**, *15*, 3069–3077.

$\text{Ta}_2\text{NiSe}_7$  is metallic and diamagnetic and undergoes no phase transitions between 4 and 300 °C, analogous to the case for  $\text{TaSe}_3$ .<sup>7</sup>

**Valence Description.** It is difficult to describe these compounds in simple valence terms. The formal assignment  $2\text{Ta}^{5+}\text{M}^{2+}\cdot 5\text{Se}^{2-}\text{Se}_2^{2-}$  is consistent with the single Se–Se bond evident in the structure. This description requires the Ta-centered bicapped trigonal prism that possesses the Se–Se bond to contain a Ta atom formally in the +5 state. To our knowledge all other Ta structures that contain Se–Se bonds are best described as having  $\text{Ta}^{4+}$  in the site with the chalcogen pair.<sup>7,19</sup> There may be some charge transfer from Se to Ta that leads to  $\text{Ta}^{4+}$  in the trigonal-prismatic site. Moreover, the majority of the Se–Se distances in the structure are between 3.1 and 3.6 Å, less than the sum of the ionic radii of two Se atoms (3.8 Å) but consistent with some extended Se–Se interactions. Thus, the metallic conduction could arise from  $\text{Ta}^{4+}$  in the bicapped-trigonal-prismatic sites, as occurs in  $\text{TaSe}_3$ .<sup>7</sup> This valence description ignores possible metal–metal interactions.

### Conclusion

Attempts to extend the chemistry of the binary Nb and Ta trichalcogenides to ternary systems have led to the synthesis of the two new layered compounds  $\text{Ta}_2\text{NiSe}_7$  and  $\text{Ta}_2\text{PtSe}_7$ . These compounds are isostructural. Their structure is similar to that of  $\text{FeNb}_3\text{Se}_{10}$ . The metallic conduction and diamagnetism of  $\text{Ta}_2\text{NiSe}_7$  is similar to that of  $\text{TaSe}_3$ . The lack of charge density wave phenomena, which are observed in the structurally related compound  $\text{FeNb}_3\text{Se}_{10}$ , suggests that the physical properties of chalcogen-rich ternary chalcogenides parallel those of the corresponding binary trichalcogenides. The description of these compounds in terms of one-dimensional chains of metal atoms is consistent with the observed physical properties. This suggests that the hypothetical compounds  $\text{Nb}_2\text{MSe}_7$  (*M* = Ni, Pd, Pt) might exhibit charge density wave phenomena. Attempts to synthesize such compounds have been unsuccessful to date.

**Acknowledgment.** This work was supported by the U.S. National Science Foundation, Solid State Chemistry (Grant DMR-83-15554). Some of the measurements were carried out in the SEM, X-ray, and magnetic susceptibility facilities of Northwestern University's Material Research Center, supported in part under the NSF-MRL program (Grant DMR82-16972).

**Registry No.**  $\text{Ta}_2\text{NiSe}_7$ , 104548-68-7;  $\text{Ta}_2\text{PtSe}_7$ , 104548-69-8; Ni, 7440-02-0; Pt, 7440-06-4; Ta, 7440-25-7; Se, 7782-49-2.

**Supplementary Material Available:** Anisotropic thermal parameters for  $\text{Ta}_2\text{NiSe}_7$  (Table III) (1 page); structure amplitudes for both compounds (Table IV) (11 pages). Ordering information is given on any current masthead page.

Contribution from the Department of Chemistry,  
University of Vermont, Burlington, Vermont 05405

## Oxidation-State-Dependent Changes in the Coordination Environment of Oxovanadium Complexes of Ethylenebis(*o*-hydroxyphenyl)glycine)

Joseph A. Bonadies and Carl J. Carrano\*

Received January 27, 1986

Oxovanadium complexes of the ligand ethylenebis(*o*-hydroxyphenyl)glycine), EHPG, have been isolated and characterized with vanadium in both the +IV and +V oxidation states. Electrochemical study of these two complexes shows that they are interrelated as opposite corners of an ECEC square mechanism (E = electron-transfer step, C = chemical step). The mechanism was investigated in several solvents, and rates were determined for the chemical steps. An oxidation-state-dependent change in the coordination environments of the complexes was identified as the process occurring in the chemical steps of the mechanism.

### Introduction

In order to better understand the interaction of vanadium with biological systems, the coordination chemistry of this element in its three accessible oxidation states (+III, +IV, and +V) with

relevant ligands needs to be explored. In light of the reported binding of vanadium to the metal-tyrosinate protein transferrin<sup>1</sup> and its interaction with the recently characterized polyphenol tunichrome, found in the vanadocytes of the tunicates,<sup>2</sup> vanadi-

\* To whom correspondence should be addressed.

(1) Harris, W. R.; Carrano, C. J. *J. Inorg. Biochem.* **1984**, *22*, 101.

(2) Bruening, R. C.; Oltz, E. M.; Furukawa, J.; Nakanishi, K.; Kustin, K. *J. Am. Chem. Soc.* **1985**, *107*, 5298.

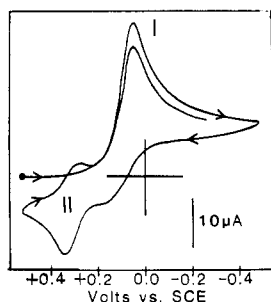
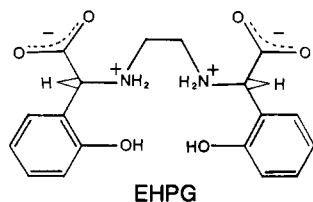


**Figure 1.** Cyclic voltammogram of an approximately 15 mM solution of compound A in methanol at a platinum electrode (25 °C, 0.1 M (TEA)Cl, 0.2 V/s).

um-phenolate chemistry seemed an appropriate starting point.

We have recently reported on the synthesis and characterization of a number of vanadium complexes of the ligand ethylenebis(*o*-hydroxyphenyl)glycine), EHPG, and its derivatives.<sup>3</sup> This



ligand was chosen for study as it had already proved useful in providing insights into the structure and chemistry of a number of iron-phenolate proteins.<sup>4,5</sup> In the course of this work two distinct oxovanadium complexes of the EHPG ligand were isolated and characterized.<sup>3</sup> These complexes were A, an octahedral oxovanadium(V) complex, utilizing two amines, two phenolates, and a carboxylate from the potentially hexadentate ligand, and B, a square-pyramidal oxovanadium(IV) complex, where two amines, a phenolate, and a carboxylate from the ligand were coordinated. The remaining uncoordinated donor groups in both complexes were shown to be in their protonated forms. Electrochemical studies revealed that compounds A and B, in contrast to other vanadium complexes of EHPG and its derivatives, displayed complicated cyclic voltammetric behavior. However, the origin of this behavior was not elucidated. We have now examined the electrochemistry of these complexes in detail, and in this report it is demonstrated that both A and B undergo oxidation-state-dependent changes in their coordination environments.

### Experimental Section

**Materials.** *meso*-[Ethylenebis(*o*-hydroxyphenyl)glycinato]oxovanadium(V) (A) and *meso*-[ethylenebis(*o*-hydroxyphenyl)glycinato]oxovanadium(IV) (B) were prepared as previously described.<sup>3</sup> UV-grade dimethylformamide (DMF) and acetonitrile (AN) were obtained from Burdick and Jackson, stored under nitrogen, and used without further purification. Methanol was stored over magnesium methoxide and distilled as needed. Tetraethylammonium hydroxide (1 M in methanol) and trifluoroacetic acid were obtained from Aldrich and used as received.

**Methods.** Cyclic voltammetric and bulk electrolysis experiments were carried out as previously described with use of a platinum-bead electrode and tetrabutylammonium hexafluorophosphate ((TBA)PF<sub>6</sub>) or tetraethylammonium chloride ((TEA)Cl) as the supporting electrolyte.<sup>3</sup> The cell was purged and kept under a blanket of solvent-saturated nitrogen gas. Double-potential-step chronoamperometry utilized a Princeton Applied Research (PAR) 175 universal programmer in conjunction with a PAR 176 potentiostat. Pulse times ranged from 1 to 3 s. Pulse voltammetry (PV) at a platinum electrode utilized a PAR 174A polarographic analyzer. All potentials are reported vs. the saturated calomel electrode (SCE) and are uncorrected for junction potentials. Electrochemical studies at low temperatures employed either a carbon tetra-

**Table I.**  $E^\circ$  Values for  $E_1$  and  $E_2^a$

step	solvent	$E^\circ$ , V	conditions
$E_1$	H <sub>2</sub> O	+0.210	pH 4.7
	MeOH	-0.003	basic <sup>b</sup>
	AN	-0.050	-22 °C
	DMF	-0.104	-22 °C
$E_2$	H <sub>2</sub> O	+0.460	pH 9.0
	MeOH	+0.305	-22 °C
	AN	+0.208	ambient <sup>c</sup>
	DMF	+0.176	ambient <sup>c</sup>

<sup>a</sup>Under conditions of high reversibility (see ref 8 for criteria). Cyclic voltammetry was used to determine the  $E^\circ$  values in all cases. The reported values have an approximate error of  $\pm 0.005$  V. <sup>b</sup>Made basic by addition of approximately 1 equiv of tetraethylammonium hydroxide. <sup>c</sup>See ref 10.

**Table II.** Chemical Step Rate Constants

step	method <sup>a</sup>	solvent	temp, °C	rate, s <sup>-1</sup>
$C_1$	DPSCA	MeOH	25	$2.3 \pm 0.1^b$
	DPSCA	DMF	25	$1.5 \pm 0.4$
	DPSCA	AN	25	$0.63 \pm 0.08$
	DPSCA	MeOH	5	$1.8 \pm 0.6$
	DPSCA	DMF	5	$0.44 \pm 0.08$
	DPSCA	AN	5	$0.39 \pm 0.04$
$C_2$	PV	MeOH	25	$3.69 \times 10^{-4}$
	PV	DMF	25	$1.34 \times 10^{-4}$
	PV	AN	25	$1.59 \times 10^{-4}$

<sup>a</sup>Legend: DPSCA = double-potential-step chronoamperometry; PV = pulse voltammetry. <sup>b</sup>At upper limit of the technique.

chloride/dry ice slush bath (-22 °C) or a circulating cold water bath (5 °C). UV-visible spectra were obtained on a Perkin-Elmer Model 553 spectrophotometer.

### Results and Discussion

The electrochemistry of the vanadium(V) species, *meso*-[ethylenebis(*o*-hydroxyphenyl)glycinato]oxovanadium(V) (A), was examined by cyclic voltammetry in a variety of solvents. The data shown were obtained in methanol (Figure 1), but virtually the same cyclic voltammetric behavior is seen in dimethylformamide and acetonitrile. In methanol, the cathodic scan reveals a reduction wave, I, at about +0.05 V. However, under ambient conditions, no reoxidation current is seen upon scan reversal. This indicates that a chemical reaction, which rapidly consumes the reduced product, follows the initial electron transfer. The product of this chemical reaction ( $C_1$ ) appears on continuing the return scan as a quasi-reversible couple, II, at +0.30 V. Continuous potential cycling causes the irreversible peak, I, to diminish with an associated increase in the peak heights of the product oxidation and reduction waves. The overall process can be described by a classical ECE mechanism:<sup>6</sup>



A return current for the reoxidation of the reduced form of A is observable by lowering the temperature of the electrochemical cell, thereby slowing the rate of the following chemical reaction. At -20 °C nearly reversible electrochemical behavior is seen in

(6) E = electron-transfer step; C = chemical step. The type of behavior described is typical of an ECE system where the chemical step generates a new electroactive species, which is reoxidized at a more positive potential. The  $E_{\text{c,irr}}$  character of the initial reduction can be demonstrated by utilizing a Nicholson and Shain type analysis (*J. Am. Chem. Soc.* **1964**, *86*, 706). A 10-fold increase in scan rate results in a 30-mV cathodic shift of the reduction peak potential (resistance effects have been ruled out). This is the behavior expected if the rate of the chemical step is fast enough to impose pure kinetic control in the cyclic voltammetry. The expected enhancement of up to 10% in the current function at slower scan rates is also observed.

(3) Bonadies, J. A.; Carrano, C. J. *J. Am. Chem. Soc.* **1986**, *108*, 4088.  
 (4) Patch, M. G.; Simolo, K.; Carrano, C. J. *Inorg. Chem.* **1983**, *22*, 2630.  
 (5) Carrano, C. J.; Spartalian, K. P.; Appa Rao, G. V. M.; Pecoraro, V. L.; Sundaralingam, M. *J. Am. Chem. Soc.* **1985**, *107*, 1651.

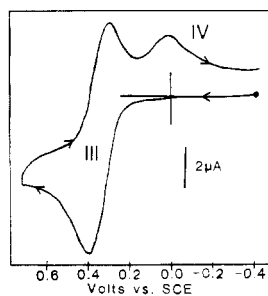


**Figure 2.** Cyclic voltammogram of compound B in methanol (approximately 3 mM, other conditions as in Figure 1).

dimethylformamide and acetonitrile although not in methanol.<sup>7</sup> The persistent irreversibility in methanol indicates that the rate of the chemical step is considerably faster in this solvent. Since these low-temperature cyclic voltammograms are nearly reversible,<sup>8</sup> the  $E^\circ$  values (given in Table I) are representative of the actual thermodynamic redox potentials.

Numerical values for the rate constant of the chemical step ( $C_1$ ) were obtained by double-potential-step chronoamperometry<sup>9</sup> with the assumption of pseudo-first-order kinetics for the process. In this technique, with an initiation at a benign potential, the electrode potential is stepped to a value where A undergoes reduction. After a short time,  $\tau$ , the electrode potential is then stepped to a value where any reduced species that has not undergone the chemical follow-up reaction undergoes oxidation back to A. The results were analyzed by the method of Schwartz and Shain<sup>9</sup> and are summarized in Table II. The rate constant of the chemical step at 25 °C in methanol was at the upper limit of the technique so data were also collected at 5 °C in all three solvents to allow comparison of the rate constants to be made in the high-confidence region of the method.

Cyclic voltammetry of complex B, *meso*-[ethylenebis(*o*-hydroxyphenyl)glycinato]oxovanadium(IV), in methanol reveals a nearly reversible redox couple, III, at +0.30 V and a small irreversible cathodic wave, IV, at approximately 0.0 V (Figure 2). The small irreversible reduction wave, IV, which only appears after cycling through III, represents the reduction of the product of a *slow* chemical reaction ( $C_2$ ) that follows the oxidation of B. The cyclic voltammetric behavior can thus be treated as an ECE system as before,<sup>10</sup> and the  $E^\circ$  values for the  $E_2$  couple in various solvents are reported in Table I.



In this case the rate of the chemical reaction ( $C_2$ ) is sufficiently slow so that rates could be conveniently measured by classical techniques. Compound B was bulk-oxidized (*vide infra*), and its conversion to product was measured by repeated pulse voltammetry. Two plateaus were visible, which corresponded to the reduction of  $B_{\text{ox}}$  and reduction of the product Y. The loss of oxidized B was monitored by measuring the current at the first

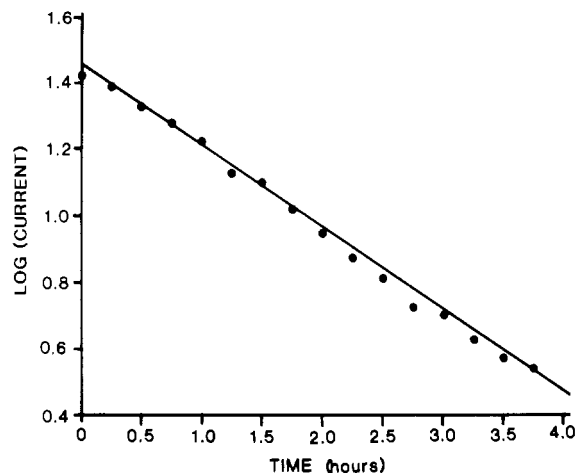


**Figure 3.** Plot of the logarithm of the current at the first plateau of the pulse voltammogram, baseline corrected, vs. time following completion of bulk oxidation of B in dimethylformamide.

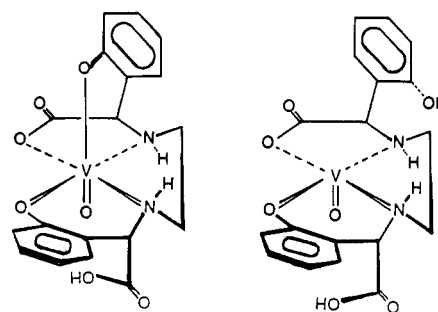
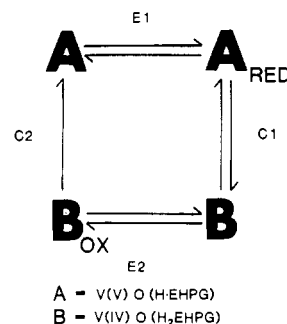


**Figure 4.** Proposed structure for compound A (right) and compound B (left).

#### Scheme I



plateau as a function of time. Complete conversion requires approximately 6 h in DMF, 3 h in AN, and 1 h in MeOH. A plot of the logarithm of the first plateau current (baseline corrected) vs. time yields a straight line (correlation coefficient greater than 0.99) in all cases, indicative of a first-order process (Figure 3). The rate constant for  $C_2$  was calculated from the slope of these plots, and the values are given in Table II.

A close inspection of the electrochemistry of both compounds A and B reveals that the same basic features are present in their cyclic voltammograms (compare Figures 2 and 3), which suggests that they may be interrelated. This hypothesis was confirmed by bulk electrolysis of both A and B. Exhaustive reduction of A consumes one electron and yields a solution whose cyclic voltammetry and UV-visible spectrum are identical with those of compound B (recall that  $C_1$  is fast). Bulk oxidation of B also involves one electron, and if sufficient time is allowed for the slower chemical follow-up reaction ( $C_2$ ) to occur, the cyclic voltammogram and optical spectrum of the product are indistinguishable from those of pure A.

Taken together, the electrochemical experiments thus far have demonstrated that compounds A and B are at opposite ends of an ECEC square system,<sup>11</sup> where two of the corners have been

- (7) The cathodic peak potential in all cases shifts to more negative values (i.e. toward its unperturbed or thermodynamic value).
- (8) Criteria used in defining electrochemical reversibility:  $i_p/v^{1/2}$  is constant, peak currents correspond to concentration changes,  $\Delta E_p$  and  $i_{pa}/i_{pc}$  values match standards (ferrocene) under the same conditions and concentrations.
- (9) Schwartz, W. M.; Shain, I. *J. Phys. Chem.* **1965**, *69*, 30.
- (10) The slow rate of the chemical step in this case results in near diffusion control of the initial electron transfer. As such, this redox couple behaves much like a reversible system, although the chemical step has observable effects on the concentration of  $B_{\text{ox}}$  at the electrode surface since  $i_{pc}/i_{pa}$  is less than 1. The irreversible product reduction wave is dependent on the rate of the chemical step. As expected, this broad product reduction peak diminishes in intensity at higher scan rates and lower temperatures as the chemical step is either outrun or suppressed. See also: Geiger, W. E., Jr. *Inorganic Reactions and Methods*; Zuckerman, J. J., Ed.; Verlag Chemie: New York, in press.

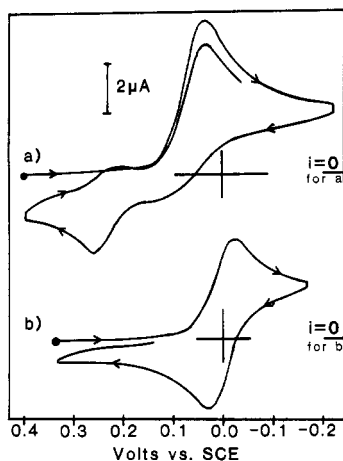


**Figure 5.** Cyclic voltammograms of (a) compound A in methanol and (b) the same system following addition of approximately 1 equiv of base. The solution is 2 mM in A, and other conditions are the same as in Figure 1.

isolated and characterized while the other two are detectable. Scheme I illustrates the process and the nomenclature of the system. The nature of the two chemical steps of this ECEC cycle is best determined by the changes necessary to close the square mechanism and the pH effects on each process.

The structures of compounds A and B are shown in Figure 4.<sup>12</sup> Since B has both a free carboxylic acid and phenol while A has only a free carboxylic acid, the "chemical" steps in our cycle would seem to be the dissociation/protonation ( $C_1$ ) and association/deprotonation ( $C_2$ ) of the phenolate ligand on the vanadium center. We can thus infer the following mechanism. The initially six-coordinate vanadium(V) complex A is reduced by one electron to form the six-coordinate vanadium(IV) species  $A_{red}$ . Dissociation of the phenolate group in the position trans to the oxo group followed by rapid protonation yields the five-coordinate species B. The dissociation is fast and is driven to the right by the fact that the resulting vanadyl ion is a softer acid and has a strong propensity toward five-coordination due to the trans-labilizing effect of the oxo group.<sup>13</sup> Compound B in its turn can be oxidized to the five-coordinate vanadium(V) species  $B_{ox}$ , which can then re-coordinate the dangling phenol, in a relatively slow step, to regenerate A.

The specific coordination isomer for A shown in Figure 4 is based on both NMR data<sup>3</sup> and knowledge of the strong trans-

labilizing effect of the oxo group, which is expected to facilitate conversion of  $A_{red}$  to B by assisting in the dissociation of the axial phenolate upon reduction. This is also consistent with the relatively rapid rate for  $C_1$ . Other coordination isomers of A, i.e. an axial carboxylate, seem less likely as they would require a coordination sphere rearrangement after loss of an equatorial phenolate in order to achieve the environment seen in B.

The pH dependence of the rate of the first chemical step,  $C_1$  (ligand dissociation), is consistent with the aforementioned mechanism. In methanol addition of base to A causes the first electrochemical step  $E_1$  to become reversible (Figure 5) by suppressing the conversion of  $A_{red}$  to B, which normally follows the initial reduction. Base favors the continued coordination of the axial phenol in  $A_{red}$ , because the phenolate anion formed by dissociation cannot be protonated and hence remains a good donor that is held in close proximity of the axial site by the stereochemistry of the ligand.

Alternatively, if base is added to a solution of B, there is a rapid conversion into  $A_{red}$ . Here deprotonation of the dangling phenol in B again favors its coordination, yielding  $A_{red}$ . In aqueous solution the generation of  $A_{red}$  from B is complete at a pH of ca. 8.8, consistent with the measured  $pK_a$  of the free phenol of B (8.0) as determined by potentiometric titration.<sup>3,14</sup> The process of interconversion of  $A_{red}$  and B via  $C_1$  is totally reversible, in the chemical sense, in aqueous and nonaqueous systems.

The chemical step  $C_2$  (ligand association) is also affected by pH, but to a lesser extent. The addition of acid slightly suppresses the rate of the  $C_2$  process and increases the reversibility of  $E_2$ , presumably by decreasing the ability of the phenol to be in its anionic form ( $pK_a > pH$ ). However, the harder vanadium(V) center, which strongly prefers six-coordination, tends to drive the reaction to completion. Base greatly accelerates the rate of  $C_2$  as it puts the free phenol in the more easily coordinated phenolate form.

## Conclusion

We have presented here an oxidation-state-dependent change in coordination environment, involving a coordination chemistry example of a well-characterized ECEC square mechanism. While such mechanisms are well-known in organometallic chemistry, they are uncommon in Werner-type complexes. These results also highlight the coordination preferences of the relatively rare oxovanadium(V) ion.

**Acknowledgment.** We wish to thank Dr. William E. Geiger for many helpful discussions and the use of his electrochemical equipment. We also wish to thank Dr. Carl A. Marrese for the introduction he provided our research group into electrochemistry. The financial support of the Research Corp. is gratefully acknowledged.

(11) The nature of an ECEC square mechanism has been recently reviewed in: Geiger, W. E. *Prog. Inorg. Chem.* **1985**, *33*, 275 and references therein.

(12) Ligand NMR and iron complex studies indicate the ligand of both A and B to be the meso isomer of EHPG (i.e. *R,S* chirality).

(13) Cotton, F. A.; Wilkinson, G. *Advanced Inorganic Chemistry*, 4th ed.; Wiley: New York, 1980.

(14) The aqueous electrochemical titration of compound B was hampered by adsorption of oxidized material at the electrode surface. Due to this, the aqueous data are treated here only qualitatively.